Synthesis and Structure−Activity Relationships of 6,7-Benzomorphan Derivatives as Use-Dependent Sodium Channel Blockers for the Treatment of Stroke

Matthias Grauert,*,† Wolf D. Bechtel,‡ Thomas Weiser,‡ Werner Stransky,† Herbert Nar,† and Adrian J. Carter§

Departments of Medicinal Chemistry and CNS Research, Boehringer Ingelheim Pharma KG, 88397 Biberach an der Riss, and Corporate Development, Boehringer Ingelheim GmbH, 55216 Ingelheim am Rhein, Germany

Received March 12, 2002

We have synthesized a series of 6,7-benzomorphan derivatives and determined their ability to bind to voltage-dependent sodium channels. We have also compared the functional consequences of this blockade in vitro and in vivo. The ability of the compounds to displace [^{3}H]batrachotoxin from voltage-dependent sodium channels was compared with their ability to inhibit [^{3}H]-glutamate release in rat brain slices and block convulsions in the maximal electroshock test in mice. We found that the hydroxyl function in the 4′-position is crucial for improving the sodium channel blocking properties. Moreover, the stereochemistry and the topology of the N-linked side chain also influence this interaction. Indeed, the affinity is improved by an aromatic substitution in the side chain. By modifying the N substituent and the substitution pattern of the hydroxyl function, we were able to discover (2*R*)-[2α,3(*S**),6α]-1,2,3,4,5,6-hexahydro-6,11,-11-tri-methyl-3-[2-(phenylmethoxy)propyl]-2,6-methano-3-benzazocin-10-ol hydrochloride. This compound was chosen as the best candidate for further pharmacological investigations.

Introduction

Thromboembolic stroke deprives the brain of an adequate supply of oxygenated blood thereby causing the death of neurons. The core area of the infarct probably dies within minutes. However, the area surrounding the core, often called the penumbra, does not die immediately. The collateralization or natural redundancy of the brain's blood supply allows this area to continue functioning with a reduced flow of blood. However, ischaemic depolarization triggers a chain reaction of electrical and chemical activity in this region, which in turn causes the release of excitatory amino acids and changes in calcium homeostasis.[1,2] If these processes are not interrupted, they will lead to cell death in the penumbra, too. Voltage-dependent Na^+ channels are thought to play a key role in ischaemic damage because blockers of such channels inhibit depolarization, thereby reducing Ca^{2+} influx through voltage-dependent calcium and NMDA receptor channels, and prevent the reversal of the Ca^{2+}/Na^+ exchanger. In addition, they should inhibit the massive nonvesicular release of excitatory amino acids that occur during ischaemia and therefore reduce excitotoxic neuronal damage.[3] Finally, it has been shown that sodium channel blockers prevent hypoxic damage to the white matter in isolated optic nerve, which is an advantage as compared to other neuroprotective agents that are active only in gray matter.[4,5] Hence, we believe strongly that sodium channel blockers should be useful for the treatment of thromboembolic stroke.[6−8]

Voltage-dependent Na^+ channels are large glycoproteins that exist as heterotrimers consisting of one 250 kDa α subunit, one 39 kDa β_1 subunit, and one 37 kDa β_2 subunit.[9−14] The α subunit is the pore-forming protein that is built up of four homologous domains of six transmembranal segments (S1−S6) and an additional membrane-associated segment between S5 and S6. This subunit contains the voltage sensor, the selectivity filter, and the inactivation gate. The two β subunits seem to have a modulatory function. They influence the amplitude of the peak sodium current and the time course of channel activation and inactivation.[15,16] In brain, five different sodium channel subtypes with high sequence homology have been cloned.[17−21]

The Na^+ channel can shift between at least three distinct conformational states—namely, resting, open, and inactivated—which determine the Na^+ channel permeability. In the resting state, the channel pore is closed, whereas in the inactivated state the channel pore is open but blocked by an internal gate. Several neurotoxins bind to distinct receptor sites on the voltage-dependent Na^+ channel and either cause blocking or opening of the channel.[22,23] Tetrodotoxin (TTX), the poison of the puffer fish, binds to the so-called neurotoxin site 1. This binding site is at the extracellular mouth of the channel. Indeed, TTX can bind to this site independently of the conformational state of the sodium channel and blocks Na^+ ion permeation.[24] Neurotoxin site 2 binds toxins such as batrachotoxin (BTX), veratridine, and aconitine, which cause persistent activation of the sodium channel.[25−27] In contrast to TTX, the binding of BTX to the sodium channel is highly dependent on the state of the channel with a strong preference for the open state. Point mutations indicated that BTX interacts with amino acids at transmembrane segment IS6 and IVS6.[28,29] Anticonvulsant and local anaesthetic

* To whom correspondence should be addressed. Tel: +49/(0)7351/54-7314. Fax: +49/(0)7351/54-5181. E-mail: Matthias.Grauert@bc.boehringer-ingelheim.com.

† Department of Medicinal Chemistry, Boehringer Ingelheim Pharma KG.

‡ Department of CNS Research, Boehringer Ingelheim Pharma KG.

§ Corporate Development, Boehringer Ingelheim GmbH.

10.1021/jm020875j CCC: $22.00
Published on Web 07/19/2002

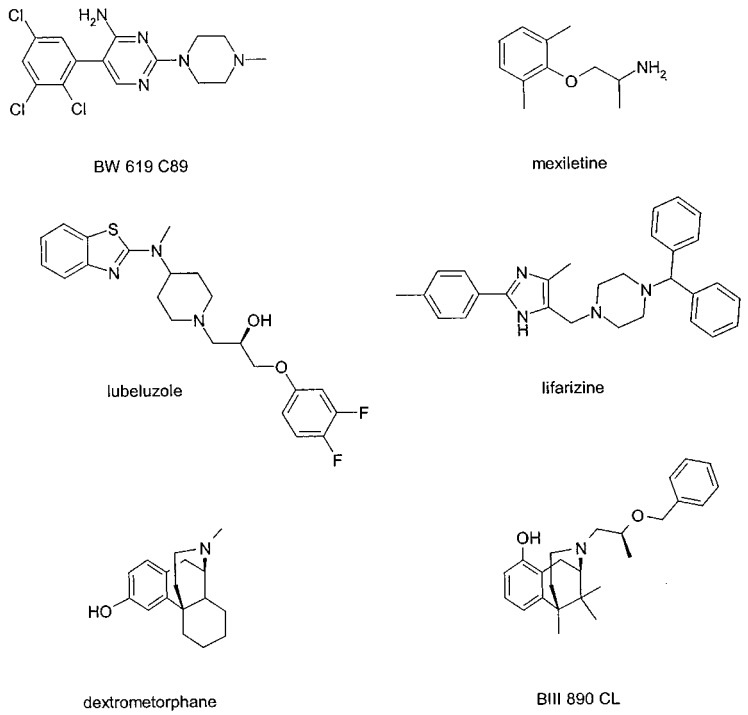

Figure 1. Use-dependent sodium channel blockers.

drugs are thought to bind to intracellular sites of the sodium channel, which share overlapping but nonidentical molecular determinants with BTX. Compounds that bind to such an internal site are thought to block the sodium channel in a use- and voltage-dependent manner. Indeed, high use dependency may be a very advantageous attribute for a voltage-dependent Na^+ channel blocker because they would preferentially block Na^+ channels in an overstimulated situation leaving physiological functions generally unaffected.

Considerable efforts have been devoted to identifying novel use-dependent sodium channel blockers that might be useful for the treatment of thromboembolic stroke. BW619C89 (Figure 1) is a sodium channel blocker that inhibits glutamate release in vitro and prevents neuronal damage after ischaemia.[30,31] Two other Na^+ channel blockers are known to possess neuroprotective activity, namely, lifarizine[32−35] and lubeluzole,[36−38] (Figure 1) and have been tested in phase II clinical trials. Unfortunately, lifarizine caused hypotension in elderly female patients[39] and clinical trials have since been discontinued. Cardiovascular side effects are perhaps indicative of the specificity problems associated with these agents: BW619C89, lubeluzole, and lifarizine all bind to different sites of classical voltage-dependent Ca^{2+} channels in addition to voltage-dependent Na^+ channels.[40] In addition, lubeluzole and lifarizine possess high affinities to a variety of different G-protein-coupled receptors.

Dextrometorphan (Figure 1) is able to block voltage-dependent sodium channels in addition to its action at the NMDA receptor channel complex and voltage-dependent Ca^{2+} channels.[41,42] We have already shown that it is possible to optimize the class of structurally related 6,7-benzomorphans for the NMDA receptor−channel complex.[43] Thus, we intended to explore 6,7-benzomorphans as a lead system for highly selective and specific blockers of the voltage-dependent sodium channel, which bind to the BTX binding site and show remarkable use dependency. In this paper, we report the synthesis of these novel compounds and we discuss their structure−activity relationships (SAR). By modification of the N substituent and the substitution pattern of the hydroxyl function, we were able to discover (2*R*)-[2α,3(*S**),6α]-1,2,3,4,5,6-hexahydro-6,11,-11-tri-methyl-3-[2-(phenylmethoxy)propyl]-2,6-methano-3-benzazocin-10-ol hydrochloride (**9a,** BIII 890 CL, Figure 1). This compound has been selected for further assessment of neuroprotective properties[44] and is currently in clinical development for thromboembolic stroke.

Chemistry

The 5,9,9-trimethyl-6,7-benzomorphan derivatives **1**, **2**, **3**, and **5** (Table 2) and their syntheses have already been described,[43] and several of the derivatives (**4** and **6**−**8**) have been synthesized according to this route. Furthermore, the synthesis of the 5,9-dimethyl-6,7-benzomorphan derivative **12** follows this path with some modifications. Thus, for these compounds, the procedure has been outlined in Scheme 1: 2-Methoxybenzyl cyanide **14** was treated with ethyl 2-bromopropionate **15**, and the intermediate imine was reduced with $NaBH_4$. Addition of ethyl acrylate to **16**, Dieckmann condensation, and subsequent decarboxylation with NaOH yields the piperidone derivative **18**. Wittig reaction with methyl triphenylphosphonium bromide and KOtBu followed by formylation with *n*-butyl formate gave **20**. Cyclization with methane sulfonic acid provided the protected benzomorphan derivative **21** as a 9:1 mixture of the 9-α and 9-*β* epimer. After deformylation, the racemic mixture was resolved into the pure 1*R*,9-α enantiomer by (+)-tartatic acid. Subsequent cleavage of the methyl ether yields **23**. The N substituent was introduced by acylation and reduction of the intermediate amide.

Scheme 1[a]

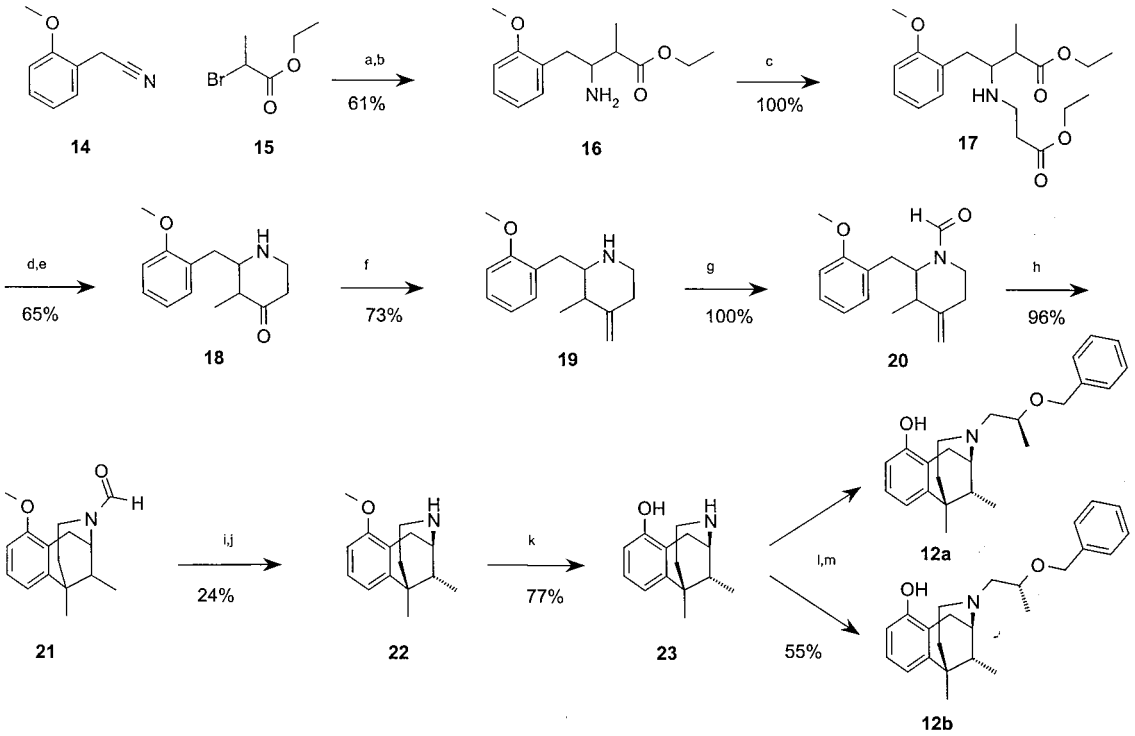

[a] Reagents: (a) Zn, CH_2Cl_2; (b) $NaBH_3CN$, EtOH; (c) CH_2=CHCOOEt, EtOH; (d) KOtBu, $C_6H_5CH_3$; (e) NaOH, EtOH; (f) Ph_3P-CH_3Br, KOtBu, THF; (g) HCOOnBu, $C_6H_5CH_3$; (h) $MeSO_3H$; (i) HCL; (j) *R*-(+)-tartaric acide; (k) HBr; (l) R″-COCl, Et_3N, CH_2Cl_2; (m) $LiAlH_4$, THF.

Table 1. Physical Characterization of New 6,7-Benzomorphan Derivatives

compd	stereo	mp[a] (°C)	$[\alpha]_D^{20}$ [b]	formula[c]
4a	(−)-1*R*,2″*S*	260	−51.2	$C_{19}H_{29}NO_2 \cdot HCl$
4b	(−)-1*R*,2″*R*	263	−86.9	$C_{19}H_{29}NO_2 \cdot HCl$
4c	(+)-1*S*,2″*S*	261	+86.1	$C_{19}H_{29}NO_2 \cdot HCl$
4d	(+)-1*S*,2″*R*	258	+51.7	$C_{19}H_{29}NO_2 \cdot HCl$
6a	(−)-1*R*	>250	−83.3	$C_{23}H_{29}NO_2 \cdot HCl$
6c	(+)-1*S*	>250	+83.9	$C_{23}H_{29}NO_2 \cdot HCl$
7a	(−)-1*R*,2″*S*	262	−77.7	$C_{24}H_{31}NO_2 \cdot HCl$
7b	(−)-1*R*,2″*R*	143[d]	−131.3	$C_{24}H_{31}NO_2 \cdot CH_4O_3S$
7c	(+)-1*S*,2″*S*	258	+77.9	$C_{24}H_{31}NO_2 \cdot HCl$
7d	(+)-1*S*,2″*R*	262	+74.6	$C_{24}H_{31}NO_2 \cdot HCl$
8a	(−)-1*R*,2″*S*	236	−26.2	$C_{25}H_{33}NO_2 \cdot HCl$
8b	(−)-1*R*,2″*R*	240	−104.6	$C_{25}H_{33}NO_2 \cdot HCl$
8c	(+)-1*S*,2″*S*	236	+103.6	$C_{25}H_{33}NO_2 \cdot HCl$
8d	(+)-1*S*,2″*R*	>240	+26.8	$C_{25}H_{33}NO_2 \cdot HCl$
9a	(−)-1*R*,2″*S*	254	−20.7	$C_{25}H_{33}NO_2 \cdot HCl$
9b	(−)-1*R*,2″*R*	245	−96.5	$C_{25}H_{33}NO_2 \cdot HCl$
9c	(+)-1*S*,2"*S*	245	+97.8	$C_{25}H_{33}NO_2 \cdot HCl$
9d	(+)-1*S*,2″*R*	256	+20.3	$C_{25}H_{33}NO_2 \cdot HCl$
10a	(−)-1*R*	253	−78.1	$C_{24}H_{31}NO_2 \cdot HCl$
11a	(−)-1*R*,2″*S*	240	−24.6	$C_{25}H_{39}NO_2 \cdot HCl$
11b	(−)-1*R*,2″*R*	140	−92.2	$C_{25}H_{39}NO_2 \cdot HCl$
12a	(−)-1*R*,9α,2″*S*	227	−13.3	$C_{24}H_{31}NO_2 \cdot HCl$
12b	(−)-1*R*,9α,2″*R*	217	−76.1	$C_{24}H_{31}NO_2 \cdot HCl$
13a	(+)-1*S*,2″*S*	246	+11.8	$C_{23}H_{29}NO_2 \cdot HCl$

[a] Melting points of the hydrochloride salts, except otherwise noted. [b] Optical rotation of the salts (c 1.0, MeOH). [c] Analyses were within 0.4% of the calculated values. [d] Methane sulfonate salt.

Synthesis of the 4′-hydroxy-5,9,9-trimethyl-6,7-benzomorphan **28** (starting material of **4** and **9**−**11**) can also be obtained as described in the literature.[42] However, cyclization of **26** with HBr gave only unsatisfactory yield (about 10%). Thus, an alternative method has been elaborated. We discovered that the use of Lewis acids is a very mild and efficient way to cyclize a piperidene derivative such as **26**. The optimal protecting group for the amino function during this process turned out to be a prior protonation. Thus, as described in Scheme 2, conversion of the piperidene **26** into the hydrogen sulfate and treatment with $AlCl_3$ resulted in 90% yield of the desired compound. Subsequent cleavage of the methyl ether by HBr gave the nor-benzomorphan derivative **28**. Enantiomeric pure nor-benzomorphan can be obtained from the corresponding pure piperidene. Thus, we resolved the piperidone **24** into the (+)-enantiomer by (+)-tartaric acid. The olefine **26** can be obtained from this material without racemization. However, under acidic conditions, **25** is sensitive to thermal racemization. Thus, after the mother liquor of the optical resolution was heated for 30 min, further (+)-enantiomer can be separated by a second crystallization. Repeating this procedure three times gave 75% overall yield of the racemic resolution.

The synthesis of the 4′-hydroxy-5-methyl-6,7-benzomorphan derivative **13a** is illustrated in Scheme 3. In a Grignard reaction, 2-methoxybenzyl chloride **30** was added to *N*-benzyl-4-methyl-pyridinium bromide **29**. Subsequent reduction with $NaBH_4$ gave **31**, which can be cyclized to the bezomorphan derivative **32** by methane sulfonic acid. Removal of both protecting groups yields **33**. Introduction of (−)-*S*-benzyloxypropionyl chloride and subsequent reduction with $LiAlH_4$ gave **13a**, which can be purified by column chromatography.

All newly synthesized compounds are listed in Table 1. Configurational assignment of these compounds has been proved by single-crystal X-ray crystallography of **9a**, **13a** (Figure 2), and BIII 277CL.[43] In general, the (−)-enantiomers of the 5,9,9-trimethyl- and 5,9-dimethyl-6,7-benzomorphan derivatives possess the 1*R* configuration. As indicated by the X-ray analysis, the

Table 2. Receptor Binding, Glutamate Release, and MES Data

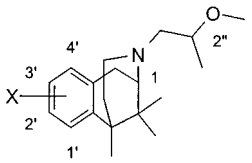

1 - 5

compd	X	stereo	[^{3}H]BTX[a] K_i (nmol/L)	[^{3}H]MK801 K_i (nmol/L)	Glu release[b] IC_{50} (nmol/L)	MES ED_{50} (mg/kg)
1a	1′-OH	(−)-1*R*,2″*S*	8990	15	>10 000 (23%)	
2a	2′-OH	(−)-1*R*,2″*S*	6010	5.6	>10 000 (29%)	0.1
3a	3′-OH	(−)-1*R*,2″*S*	>10 000 (45%)	7.1	>10 000 (21%)	0.7
4a	4′-OH	(−)-1*R*,2″*S*	783	39	3190	1.0
4b	4′-OH	(−)-1*R*,2″*R*	3310	132	4153	0.8
4c	4′-OH	(+)-1*S*,2″*S*	∼10 000 (52%)	>1000	>10 000 (25%)	
4d	4′-OH	(+)-1*S*,2″*R*	∼10 000 (48%)	>1000	>10 000 (42%)	
5a	H	(−)-1*R*,2″*S*	4700	16	∼10 000 (52%)	
dextrometorphan			4800		>10 000 (5%)	
mexiletine			22 700		47 000	
BW619			4000		17 850	
lubeluzole			203		2939	
lifarizine			259		494	

[a] K_i or percent inhibition at 10 000 nmol/L. [b] IC_{50} or percent inhibition at 10 000 nmol/L.

Scheme 2[a]

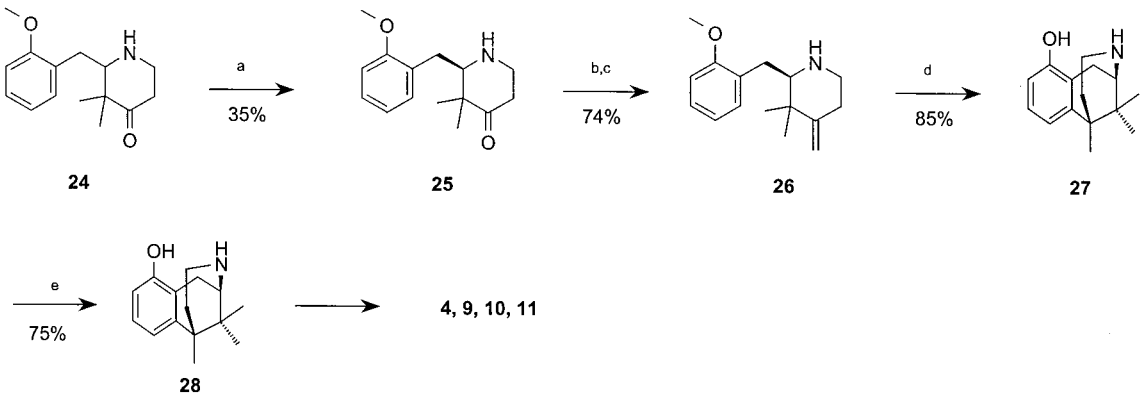

[a] Reagents: (a) *R*-(+)-tartaric acide; (b) $Ph_3P{-}CH_3Br$, KOtBu, THF; (c) H_2SO_4; (d) $AlCl_3$, CH_2Cl_2; (e) HBr.

5-methyl-4′-hydroxy-6,7-benzomorphan derivative **13a** had the 1*S* configuration and showed a positive sign in optical rotation. However, the change in configurational assignment is only due to nomenclature rules and in the case of **13a** the *S* configuration possesses the same topology as the 1*R* isomers of the 5,9,9-trimethyl- and 5,9-dimethyl-6,7-benzomorphan derivatives.

Biological Activity and Discussion

We have evaluated a series of benzomorphan derivatives for their ability to displace [^{3}H]BTX from the sodium channel binding site in synaptosomal preparations of rat cerebral cortex. Furthermore, we studied the effects of these compounds on the veratridine-induced release of glutamate from rat brain slices. The maximum electroshock (MES) test in mice was used to assess anticonvulsive activity in vivo. The results are summarized in Tables 2 and 3. In addition, the affinity for the BTX binding site was correlated with the ability to inhibit veratridine-induced glutamate release ($n = 26$, $r^2 = 0.73$, $p < 0.001$, Figure 3), an observation that indicates that the compounds under evaluation are indeed functional blockers of the voltage-dependent sodium channel.

To analyze SAR of benzomorphan derivatives at the voltage-dependent sodium channel, we initially evaluated the relevance of the aromatic hydroxyl function. Using the N-2-methoxypropyl benzomorphan derivatives, which we have discovered during our NMDA channel program, we observed that a hydroxyl function in the 4′-position is crucial for improving the sodium channel blocking properties. In addition, stereochemistry of the benzomorphan and the topology of the side chain seem to be important factors for enhancing this interaction. As indicated in Table 2, only the 1*R*,2″*S* enantiomer **4a** of the four stereoisomeric 4-hydroxy-5,9,9-tetramethyl-6,7-benzomorphans exhibited a notable affinity. In a second series, we estimated the influence of the N substitution on the affinity to the sodium channel. As demonstrated by compounds **6**−**8** (Table 3), the affinity at the sodium channel can be improved by an aromatic substitution in the side chain. The optimal distance between the aromatic substitution and the nitrogen seems to be 3−4 atoms. The combination of an optimized side chain with the best benzomorphan system resulted in **9a**, which gave a further improvement in affinity at the BTX binding site as well as progress in inhibiting the veratridine-induced gluta-

Scheme 3[a]

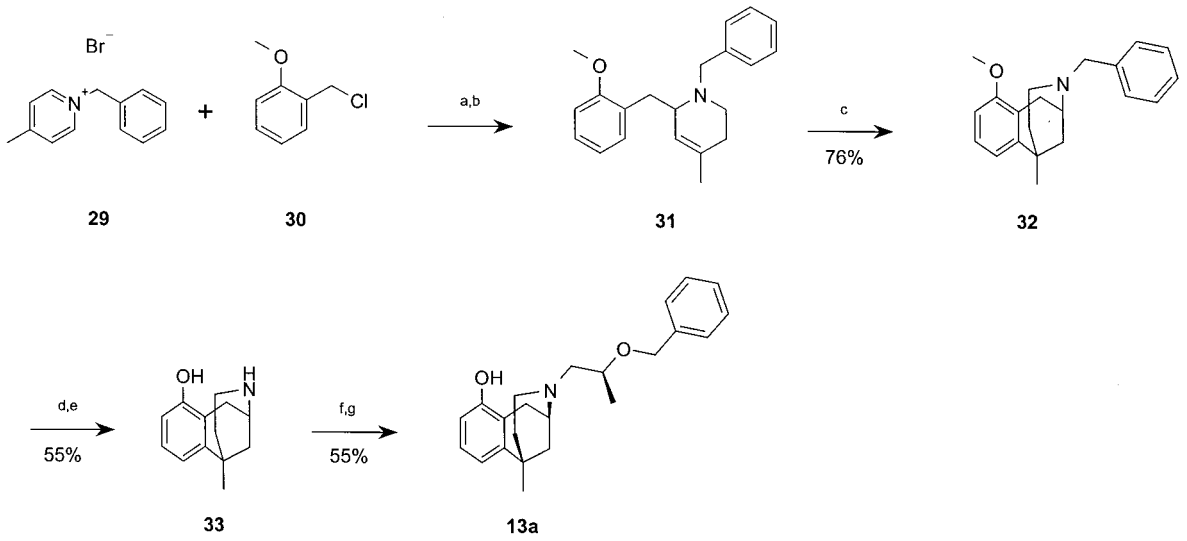

[a] Reagents: (a) Mg, Et_2O; (b) $NaBH_4$; (c) $MeSO_3H$; (d) Pd/C, MeOH; (e) HBr; (f) R″-COCl, Et_3N, CH_2Cl_2; (g) $LiAlH_4$, THF.

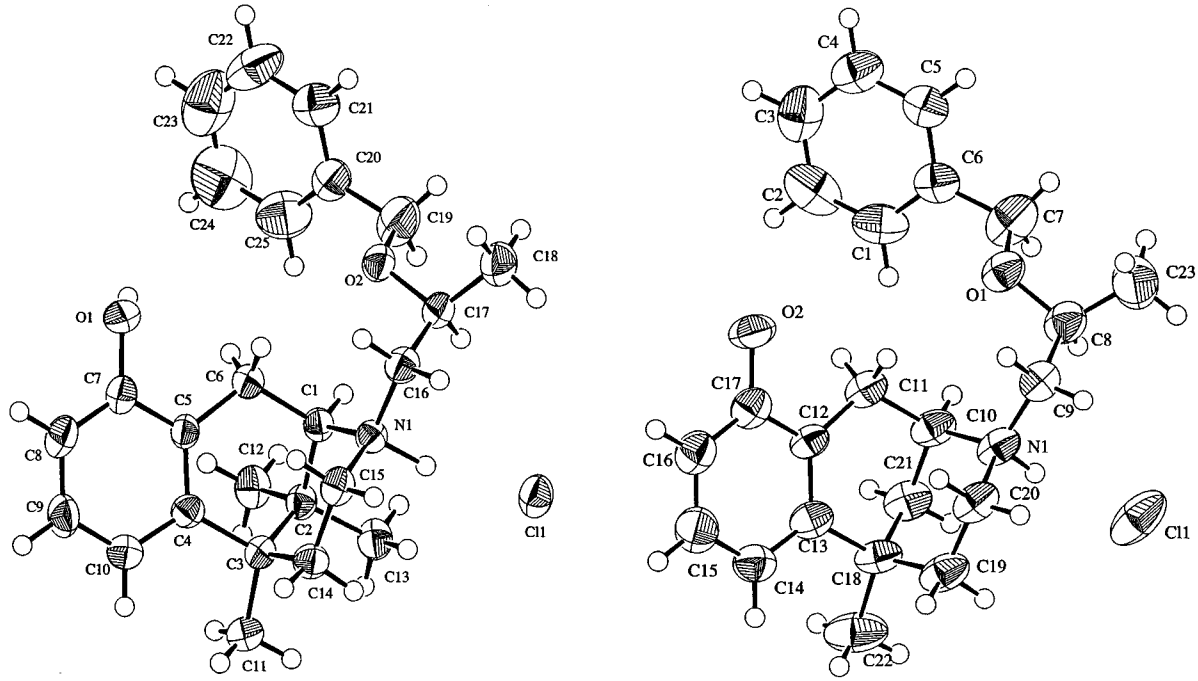

Figure 2. X-ray structure of compounds **9a** and **13a** (thermal ellipsoids drawn at the 50% probability level).

mate release. Comparison of **9a** with the corresponding derivative **10a** indicated that the chiral center of the side chain does not contribute to the improved binding affinity at the BTX binding site. Nevertheless, this chiral center is crucial for the specificity of these compounds for the sodium channel. As indicated in Table 4, **10a** has almost identical affinity for the verapamil binding site of the L type calcium channel as for the BTX site, whereas the diastereomer **9b** loses affinity at the sodium channel. In contrast, the two cyclohexyl-substituted derivatives **11a**,**b** did not show this stereo differentiation. Indeed, this is in agreement with the observation that the aromatic structure of the side chain interacts with the binding site of the sodium channel protein. The 9-desmethyl derivatives **12a** and **13a** gave almost identical affinities as **9a** at the BTX binding site. This observation reveals that the 9-methyl or the 9,9-dimethyl substitution is not crucial for an interaction of the benzomorphan derivatives with the sodium channel. In summary, SAR indicated that apart from the nitrogen functionality of the benzomorphan system, the hydroxy function and the aromatic side chain are the most important elements of the structure for its interaction with the sodium channel protein.

In addition to the in vitro evaluation of the novel sodium channel blockers, we investigated the ability of these compounds to inhibit convulsions after MES in mice. Sodium channel blockers are known to demonstrate potent anticonvulsant activity in this model, and we have used this model to show that our compounds pass through the blood−brain barrier. The compounds were administered subcutaneously 15 min before applying an electroshock via eye electrodes. The ability to inhibit tonic seizures in the MES test correlated with

Table 3. Receptor Binding, Glutamate Release, and MES Data

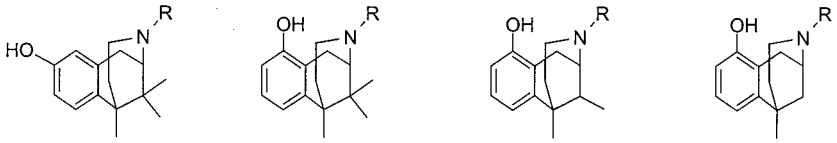

6 - 8 9 - 11 12 13

compd	R	stereo	[^{3}H]BTX K_i (nmol/L)	Glu release IC_{50} (nmol/L)	MES[a] ID_{50} (mg/kg)
6a	$(CH_2)_2-Ph$	(−)-1*R*	1060	3000	
6c	$(CH_2)_2-Ph$	(+)-1*S*	1290	5029	
7a	$CH_2CH(OPh)Me$	(−)-1*R*,2″*S*	149	5779	>30 (0%)
7b	$CH_2CH(OPh)Me$	(−)-1*R*,2″*R*	662	6024	
7c	$CH_2CH(OPh)Me$	(+)-1*S*,2″*S*	1530	6464	>100 (0%)
7d	$CH_2CH(OPh)Me$	(+)-1*S*,2″*R*	864	6340	
8a	$CH_2CH(O\ CH_2Ph)Me$	(−)-1*R*,2″*S*	312	2300	10.1
8b	$CH_2CH(O\ CH_2Ph)Me$	(−)-1*R*,2″*R*	382	3177	35.3
8c	$CH_2CH(O\ CH_2Ph)Me$	(+)-1*S*,2″*S*	1870	4516	>100 (30%)
8d	$CH_2CH(O\ CH_2Ph)Me$	(+)-1*S*,2″*R*	1230	2676	>100 (30%)
9a	$CH_2CH(O\ CH_2Ph)Me$	(−)-1*R*,2″*S*	43	322	6.1
9b	$CH_2CH(O\ CH_2Ph)Me$	(−)-1*R*,2″*R*	114	922	9.4
9c	$CH_2CH(O\ CH_2Ph)Me$	(+)-1*S*,2″*S*	1331	1289	>100 (40%)
9d	$CH_2CH(O\ CH_2Ph)Me$	(+)-1*S*,2″*R*	1494	3772	>100 (40%)
10a	$CH_2CH_2\ O\ CH_2Ph$	(−)-1*R*	20	379	2.1
11a	$CH_2CH(O\ CH_2cHex)Me$	(−)-1*R*,2″*S*	208	975	>30 (0%)
11b	$CH_2CH(O\ CH_2cHex)Me$	(−)-1*R*,2″*R*	241	1481	>30 (0%)
12a	$CH_2CH(O\ CH_2Ph)Me$	(−)-1*R*,9α,2″*S*	54	134	2.4
12b	$CH_2CH(O\ CH_2Ph)Me$	(−)-1*R*,9α,2″*R*	153	452	3.1
13a	$CH_2CH(O\ CH_2Ph)Me$	(+)-1*S*,2″*S*	47	255	2.2

[a] ID_{50} or percentage of animals that did not develop tonic convulsion at indicated dose.

Table 4. Comparison of the Specificity of Different Benzomorphan Derivatives for the Sodium Channel

binding site	K_i (nmol/L) 9a	9b	10a
Na^+ (BTX)	43	114	20
Na^+ (TTX)	>10 000	>10 000	>10 000
Ca^{2+} (DHP)	>10 000	>10 000	>10 000
Ca^{2+} (verapamil)	449	500	60
Ca^{2+} (diltiazem)	660	391	217

the affinity of the benzomorphan derivatives for the BTX binding site ($r^2 = 0.62$, $p < 0.05$, Figure 4) and with the ability to inhibit the veratridine-induced glutamate release ($r^2 = 0.78$, $p < 0.01$, Figure 4). We excluded compounds **2a**−**4b** a priori from this correlation because these compounds also bind to the NMDA receptor channel complex (Table 1). Keeping this in mind, the correlation demonstrates that affinity for the sodium channel or functional blockade of the channel is indeed an essential factor in determining the in vivo activity of the compounds under evaluation. The correlation of MES effect with glutamate release inhibition is slightly better than MES effect with BTX affinity. This is in agreement with the assumption that functional effects in brain slices translate better to an in vivo effect than binding measured in synaptosomal preparations.

Compounds **2a**−**4b** are very effective in the MES test, probably due to their additional high affinity to the NMDA receptor channel complex (Table 1). Indeed, NMDA receptor channel blockers have attracted a great deal of attention because of their therapeutic potential in the treatment of stroke.[45,46] However, NMDA receptor antagonists possess several drawbacks. They have a narrow therapeutic window, do not prevent the initial depolarization or massive release of excitatory amino

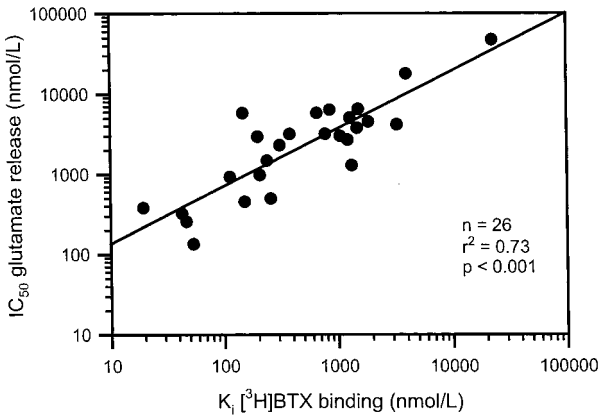

Figure 3. Correlation of BTX binding affinity with the ability to inhibit veratridine-induced glutamate release for various sodium channel blockers.

acids, and do not act neuroprotectively in the white matter of the brain. However, we know that human stroke encompasses both white and gray matter. Furthermore, it has been shown that sodium channel blockers such as TTX and saxitoxin prevent anoxic damage in mammalian white matter.[47] Therefore, our interest has been focused on specific blockers of voltage-dependent sodium channels as an alternative.

On the basis of the highest affinity and specificity for the sodium channel as well as a favorable in vivo activity in the MES test, we have selected **9a** (BIII 890 CL) for further pharmacological investigations. With an affinity of 43 nmol/L for the BTX site, **9a** is indeed one of the most potent compounds at this binding site. Furthermore, we demonstrated very high specificity on the basis of more than 65 other binding sites[44] for this compound. We believe that this is a crucial advantage

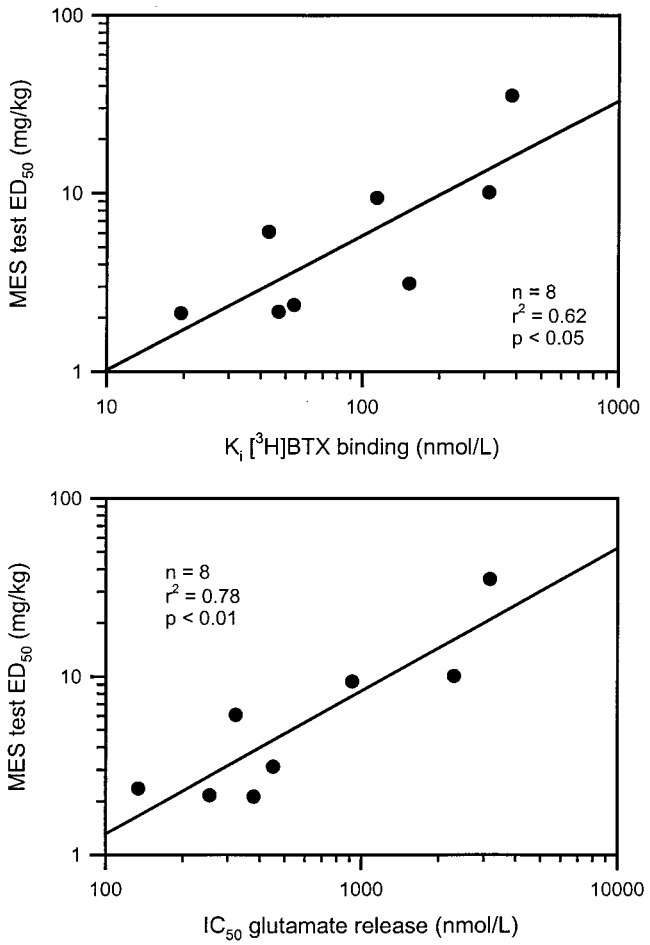

Figure 4. Correlation of BTX binding affinity and the capability to inhibit veratridine-induced glutamate release, respectively, with the ability to suppress tonic seizures after maximum electrical shock in mice for various 6,7-benzomorphan derivatives.

because almost all sodium channel blockers hitherto clinically tested are weak, unspecific, or do not discriminate between resting and inactivated states at the sodium channel. However, compounds that bind selectively to the BTX binding site should discriminate very well between different states of channel activation because this site is only available for a drug in the open or inactivated state. As demonstrated recently for the MK-801 binding site of the NMDA receptor channel complex,[48] use dependency should increase with affinity of compounds to such an internal binding site of the channel protein. Indeed, electrophysiological experiments demonstrated that **9a** shows a remarkable discrimination between channel states and a very high use dependency in achieving steady state channel blockade. Thus, we anticipate that the compound will preferentially block sodium channels in pathophysiological situations such as stroke where the channel is depolarized. In contrast, healthy neurons with physiological membrane potentials should not be pronouncedly affected. Finally, we have demonstrated that BIII 890 CL is active in models of focal ischemia in doses that did not induce side effects such as disturbance of motor coordination or effects at the cardiovascular system. The clinical development of BIII 890 CL for the indication of stroke is in progress.

Experimental Section

Chemistry. ^{1}H nuclear magnetic resonance (NMR) spectra were recorded with a Bruker AM250 spectrometer. Chemical shifts are reported as values (ppm) relative to internal tetramethylsilane. Melting points were obtained in a Büchi 510 apparatus and are uncorrected. Elemental analyses were obtained from the Analytical Department of the Boehringer Ingelheim KG. Silica gel 60, 230−400 mesh, was used for flash chromatography. Optical rotations were measured on a Perkin-Elmer 241 polarimeter.

Ethyl 3-Amino-4-(2-methoxyphenyl)-2-methylbutyrate (16). Trimethylsilyl chloride (15 mL) was added to a slurry of zinc (150 g, 2.3 mol) in dichloromethane (1.5 L) and stirred at ambient temperature under nitrogen. After 30 min, trahydrofuran (THF, 900 mL) was added, the slurry was heated to 42 °C, and a mixture of ethyl 2-bromopropionate (362 g, 2.0 mol) and 2-methoxybenzyl cyanide (147 g, 1.0 mol) was added. The mixture was heated for 2 h at reflux temperature and subsequently cooled to 5 °C, and the excess of zinc was removed by filtration. Sodium borohydride (70 g, 1.8 mol) was added, and 250 mL of ethanol was added cautiously. After 3 h, 1 L of 2 N hydrochloric acid was added and the phases were separated. The aqueous phase was extracted two times with dichloromethane (200 mL). The combined organic phase was dried, and the solvent was removed in vacuo. To the residue, 400 mL of toluene was added, cooled, and alkalized with concentrated ammonia. The phases were separated, and the aqueous phase was extracted twice with 400 mL of toluene. The combined organic phase was dried, and the solvent was removed in vacuo to give 149 g (61%) of **16** as an oil (2:1 diastereomeric mixture). ^{1}H NMR ($CDCl_3$): δ 1.25 (m, 6H), 2.38−2.64 (m, 2H), 2.81 and 2.98 (2dd, 1H, J = 4.3, 11 Hz), 3.17 and 3.38 (2m, 1H), 3.80 (s, 3H), 4.14 (q, 2H, J = 7.5 Hz), 6.77−7.26 (m, 4H).

Ethyl 3-(2-Ethoxycarbonylethyl)amino-4-(2-methoxyphenyl)-2-methylbutyrate (17). A solution of **16** (148 g, 0.6 mol) and ethyl acrylate (119 g, 1.2 mol) in 250 mL of ethanol was heated for 6 h under reflux. The solvent was removed in vacuo, and 300 mL of toluene was added to the residue and again removed in vacuo to give 210 g (99.6%) of **17** as an oil.

2-(2-Methoxyphenyl)methyl-3-methyl-4-piperidone (18). Potassium *tert*-butoxide (80 g, 0.7 mol) was added to a solution of **17** (210 g, 0.6 mol) in 3 L of toluene, and the mixture was heated for 40 min at reflux temperature while the formed ethanol was distilled off. The solvent was removed in vacuo, 400 mL of ethanol and 200 mL of a 40% aqueous solution of NaOH were added to the residue, and the mixture was heated for 3 h under reflux. The alcohol was removed in vacuo, and the water phase was extracted three times with ether. The organic phase was dried and filtered, and the solvent was removed in vacuo to give 91.2 g (65.4%) of **18** as an oil.

2-(2-Methoxyphenyl)methyl-3-methyl-4-methenylpiperidine Oxalate (19). Potassium *tert*-butoxide (6.3 g, 56 mmol) was added to a suspension of methyltriphenylphosphonium bromide (20.1 g, 56 mmol) in 150 mL of THF under nitrogen. After it was stirred at 40 °C for 30 min, the mixture was allowed to cool to ambient temperature and a solution of **18** (11.0 g, 47 mmol) in 50 mL of THF was added. After 1 h at ambient temperature, the solution was cooled and 50 mL of ice water was added. THF was removed in vacuo, and the residue was extracted twice with 50 mL of dichloromethane. The organic phase was dried and filtered, and the solvent was removed in vacuo. The residue was dissolved in acetone, and oxalic acid was added to give 11.1 g (73%) of **19** as a salt; mp 144−145 °C. ^{1}H NMR ($CDCl_3$): δ 1.29 (d, 3H, J = 6.5 Hz), 2.33−3.45 (m, 8H), 3.86 (s, 3H), 4.96 (s, 1H), 5.02 (s, 1H), 5.03 (s, 1H), 6.84−7.33 (m, 4H).

1-Formyl-2-(2-methoxyphenyl)methyl-3-methyl-4-methenylpiperidine (20). A solution of **19** (8.0 g, 35 mmol; after previous liberation of the base from the oxalic acid salt) in 30 mL of butylformate was refluxed for 4 h. The solvent was removed in vacuo to give 9.2 g (100%) of **20** as an oil. The product is a 2:1 diastereomeric mixture. ^{1}H NMR ($CDCl_3$): δ 1.09 (d, 3H, J = 6.5 Hz), 2.02−3.68 (m, 7H), 4.36 and 4.78

(2m, 1H), 3.81 and 3.82 (2s, 3H), 4.86 (s, 1H), 4.89 (s, 1H), 6.76−7.31 (m, 4H), 7.66 and 8.02 (2s, 1H).

***N*-Formyl-2′-methoxy-5,9-dimethyl-6,7-benzomorphan (21).** A solution of **20** (5.0 g, 19 mmol) in 30 mL of methane sulfonic acid was heated at 100 °C for 45 min. The solution was cooled and poured into 100 mL of ice water and extracted twice with ethyl acetate (50 mL). The combined organic phases were washed with 20 mL of a 10% aqueous solution of K_2CO_3, dried, and filtered, and the solvent was removed in vacuo to give 4.8 g (96%) of **21** as an oil. The product is a 9:1 mixture of the 9-α and 9-*β* diastereomere. ^{1}H NMR ($CDCl_3$): *δ* 0.81 (d, 3H, *J* = 6.2 Hz), 1.34 and 1.39 (2s, 3H), 1.36−3.39 (m, 7 H), 3.87 (s, 3H), 4.76 and 4.78 (2m, 1H), 6.66−7.26 (m, 3H), 8.02 and 8.28 (2s, 1H).

(−)-(1*R*,9α)-2′-Methoxy-5,9-dimethyl-6,7-benzomorphan Tartrate (22). A solution of **21** (4.8 g, 18.5 mmol) in 50 mL of propanol and 50 mL of hydrochloric acid (32%) was refluxed for 8 h. The solvent was removed in vacuo, and 50 mL of water was added to the residue and washed with 50 mL of toluene. Afterward, the water solution was alkalized with 5 g of K_2CO_3 and twice extracted with 100 mL of ethyl acetate. The combined organic phase was dried and filtered, and the solvent was removed in vacuo. The residue was dissolved in 40 mL of ethanol, and *R*-(+)-tartaric acid (2.8 g, 18.7 mmol) was added. The resulting precipitate was filtered off and recrystallized twice from methanol to give 1.7 g (24%) of **22**; mp 234−236 °C. ^{1}H NMR ($CDCl_3$): of the base *δ* 0.81 (d, 3H, *J* = 6.5 Hz), 1.36 (s, 3H), 1.88 (s, 1H), 1.34−3.05 (m, 7H), 3.15 (m, 1H), 3.83 (s, 3 H), 6.69 (d, 1H, *J* = 8.4 Hz), 6.87 (d, 1H, *J* = 8.4 Hz), 7.16 (t, 1H, *J* = 8.4 Hz).

(−)-(1*R*,9α)-2′-Hydroxy-5,9-dimethyl-6,7-benzomorphan Hydrobromide (23). A solution of **22** (1.5 g, 6.5 mmol) in 15 mL of hydrobromic acid (48%) was refluxed for 2 h. The solvent was removed in vacuo, and 15 mL of THF was added to the residue. The resulting amorphic precipitate was filtered off to give 1.5 g (77%) of **23** as the hydrobromic salt.

(−)-(1*R*,9α,2″*S*)-2-(2-Benzyloxypropyl)-1′-hydroxy-5,9-dimethyl-6,7-benzomorphan Hydrochloride (12a). A solution of *S*-(−)-2-benzyloxypropionyl chloride (1.1 g, 5.5 mmol) in 10 mL of dichloromethane was added to a solution of **23** (0.75 g, 2.5 mmol) and *N*-methylmorpholine (3 mL) in 15 mL of dichloromethane at 0 °C. The solution was stirred for 0.5 h at 0 °C and for 0.5 h at ambient temperature. Thereafter, 20 mL of 2 N HCl was added, the organic phase was separated and dried, and the solvent was removed in vacuo. The residue was dissolved in 25 mL of THF, and $LiAlH_4$ (0.5 g) was added. After 1 h, water (2 mL) and a saturated solution of ammonium tartrate (10 mL) were added. The organic phase was separated, and the aqueous layer was extracted with ethyl acetate (3 × 60 mL). The organic phases were combined, dried, and filtered, and the solvent was removed in vacuo. The residue was dissolved in ether and converted to the hydrochloride salts using ethereal hydrogen chloride to give 0.6 g of **12a** (55%); mp 226−227 °C; $[\alpha]_D^{20} = -13.3°$ (c 1.0, MeOH). ^{1}H NMR (CD_3-OD): *δ* 0.82 (d, 3H, *J* = 7.2 Hz), 1.33 (d, 3H, *J* = 7.2 Hz), 1.40 (s, 3H), 1.42−4.17 (m, 10H), 4.50 (d, 1H, *J* = 14.2 Hz), 4.75 (d, 1H, *J* = 14.2 Hz), 6.68 (d, 1 H, *J* = 8.4 Hz), 6.80 (d, 1H, *J* = 8.4 Hz), 7.07 (t, 1H, *J* = 8.4 Hz), 7.26−7.50 (m, 5H). Anal. ($C_{24}H_{31}NO_2$·HCl) C, H, N.

(−)-(1*R*,9α,2″*R*)-2-(2-Benzyloxypropyl)-1′-hydroxy-5,9-dimethyl-6,7-benzomorphan Hydrochloride (12b). Compound **12b** was prepared in an analogous manner; mp 216−217 °C; $[\alpha]_D^{20} = -76.1°$ (c 1.0, MeOH). ^{1}H NMR (CD_3OD): *δ* 0.81 (d, 3H, *J* = 7.4 Hz), 1.33 (d, 3H, *J* = 6.2 Hz), 1.40 (s, 3H), 1.43−3.61 (m, 9H), 4.06 (m, 1H), 4.52 (d, 1H, *J* = 14.0 Hz), 4.74 (d, 1H, *J* = 14.0 Hz), 6.69 (d, 1 H, *J* = 8.4 Hz), 6.81 (d, 1H, *J* = 8.4 Hz), 7.08 (t, 1H, *J* = 8.4 Hz), 7.26−7.50 (m, 5H). Anal. ($C_{24}H_{31}NO_2$·HCl) C, H, N.

(+)-(2*R*)-2-(2-Methoxyphenyl)methyl-3,3-dimethyl-4-piperidone Tartrate (25). A solution of **24** (which has been prepared according to the method described for **18**) (450 g, 1.8 mol) in 1.5 L of acetone was treated with a solution of *S*-(−)-tartaric acid (273 g, 1.8 mol) in 0.5 L of water. After 30 min, the resulting precipitate was filtered off and recrystallized from water to give 249.8 g (35%) of **25**; mp 151−152 °C; $[\alpha]_D^{20} = +26.3°$ (c 1.0, water). ^{1}H NMR ($CDCl_3$): of the base *δ* 1.20 (s, 3H), 1.23 (s, 3H), 1.68 (br s, 1H), 2.03−3.08 (m, 6H), 3.20 (m, 1H), 3.81 (s, 3H), 6.77−7.28 (m, 4H). The mother liquor was heated for 4 h under reflux to achieve racemization. After it was cooled, the resulting precipitate was filtered off and was recrystallized to obtain further **25**.

(+)-(2*R*)-2-(2-Methoxyphenyl)methyl-3,3-dimethyl-4-methenylpiperidine Hydrosulfate (26). Compound **26** was prepared in analogy to **19** and isolated as the sulfuric acid salt; mp 215−216 °C; $[\alpha]_D^{20} = +73.7°$ (c 1.0, MeOH). ^{1}H NMR (CD_3-OD): *δ* 1.25 (s, 3H), 1.36 (s, 3H), 2.33−3.44 (m, 7H), 3.86 (s, 3H), 4.97 (s, 1H), 5.00 (s, 1 H), 6.84−7.38 (m, 4H).

(−)-(1*R*)-2′-Methoxy-5,9-dimethyl-6,7-benzomorphan Tartrate (27). A suspension of **26** (5.9 g, 20 mmol) and 9 g of $AlCl_3$ in 6 mL of dichloromethane was refluxed for 2 h (temperature of the mixture 46−47 °C). The suspension was cooled, and 50 mL of dichloromethane and 100 g of ice were added. After addition of 200 mL of NaOH (10% aqueous solution), the organic phase was separated, dried, and filtered, and the solvent was removed in vacuo. The residue was dissolved in 20 mL of MeOH, and *R*-(+)-tartaric acid (3.1 g, 20.7 mmol, dissolved in 2 mL of hot water) was added. The resulting precipitate was diluted with 50 mL of acetone and filtered off to give 6.7 g (85%) of **27**; mp 236−238 °C. ^{1}H NMR (CD_3OD): *δ* 0.92 (s, 3H), 1.35 (s, 3H), 1.36 (m, 1H), 1.41 (s, 3H), 2.25 (m, 1H), 2.69−3.22 (m, 4H), 3.57 (m, 1H), 3.87 (s, 3H), 4.43 (s, 2H), 6.89 (d, 1H, *J* = 8.5 Hz), 7.03 (d, 1H, *J* = 8.5 Hz), 7.28 (t, 1H, *J* = 8.5 Hz).

(−)-(1*R*)-2′-Hydroxy-5,9-dimethyl-6,7-benzomorphan Hydrobromide (28). Compound **28** was prepared as described for **23**; mp > 250 °C; $[\alpha]_D^{20} = -52.4°$ (c 1.0, MeOH). ^{1}H NMR ($CDCl_3$): of the base *δ* 0.85 (s, 3H), 1.24 (s, 3H), 1.30 (s, 3H), 1.06−3.24 (m, 7 H), 6.56 (d, 1H, *J* = 6.9 Hz), 6.75 (d, 1H, *J* = 6.9 Hz), 6.90 (br, 2H), 6.96 (t, 1H, *J* = 6.9 Hz).

***N*-Benzyl-2-(2-methoxyphenyl)methyl-4-methyl-2-piperidene (31).** A solution of 2-methoxybenzyl chloride (31.3 g, 0.20 mol) in 100 mL of ether was added to a slurry of Mg (6.0 g, 0.25 mol) in 50 mL of ether and stirred under reflux. After 1 h, the resulting solution was added to a cooled slurry of *N*-benzyl-4-methyl-pyridinium bromide (52.8 g, 0.20 mol) and stirred for 2.5 h at −10 °C. The mixture was quenched with 100 mL of ammonia chloride solution, the organic phase was separated and dried, and the solvent was removed in vacuo. The residue was dissolved in 250 mL of methanol and $NaBH_4$ (9.5 g, 0.25 mol), and 20 mL of 2 N NaOH was added and stirred for 12 h at room temperature. Subsequently, methanol was removed in vacuo, and the residue was extracted two times with 100 mL of ethyl acetate. The combined organic phase was washed with 50 mL of water, and the solvent was removed in vacuo. The residue was dissolved in 200 mL of 2 N HCl and extracted two times with 50 mL of ethyl acetate, and the water solution was neutralized with NaOH and two times extracted with 150 mL of ethyl acetate. The organic solvent was dried, and after it was filtered, the solvent was removed in vacuo to give 31 g of **31** as a crude oil.

2-Benzyl-2′-methoxy-5-methyl-6,7-benzomorphan Oxalate (32). A solution of **31** (30.8 g, 100 mmol) in 100 mL of methane sulfonic acid was heated at 100 °C for 2 h. The solution was cooled and poured into 300 mL of ice water, alkalized with ammonia, and extracted twice with 250 mL of ethyl acetate. The combined organic phase was dried and filtered, and the solvent was removed in vacuo. The residue was dissolved in 1 L of MeOH, heated with charcoal, and filtered over silica gel. The solvent was removed in vacuo, and the residue was dissolved in ether and treated with oxalic acid to give 30.1 g (76%) of **32** as the oxalate; mp 149−152 °C. ^{1}H NMR (CD_3OD): *δ* 1.46 (s, 3H), 1.55−3.50 (m, 8H), 3.88 (s, 3H), 3.91 (m, 1H), 4.44 (s, 2H), 6.87 (d, 1H, *J* = 8.5 Hz), 7.00 (d, 1H, *J* = 8.5 Hz), 7.23 (t, 1H, *J* = 8.5 Hz), 7.40−7.59 (m, 5H).

2′-Hydroxy-5-methyl-6,7-benzomorphan Hydrobromide (33). A solution of **32** (30 g, 75 mmol) in 600 mL of MeOH was mixed with Pd/C (10%, 3 g) and hydrogenated at 60 °C and 5 bar for 2.5 h. Subsequently, 3.4 L of MeOH was added, the mixture was heated, and the catalyst was filtered off. After it was cooled, the crystalline material was filtered and the solution was concentrated until further material crystallized. After it was cooled, these crystals were also

separated, the combined material was dissolved in 80 mL of hydrobromic acid (48%), and it was refluxed for 6 h. The solvent was removed in vacuo, and acetone was added to the residue. The resulting precipitate was filtered off to give 11.7 g (55%) of **33** as the hydrobromic salt; mp 226−228 °C. ^{1}H NMR (CD_3OD): δ 1.44 (s, 3H), 1.56−3.21 (m, 8H), 4.06 (m, 1H), 6.67 (d, 1H, J = 8.5 Hz), 6.87 (d, 1H, J = 8.5 Hz), 7.06 (t, 1H, J = 8.5 Hz).

(+)-(1*S*,2″*S*)-2-(2-Benzyloxypropyl)-1′-hydroxy-5,9-dimethyl-6,7-benzomorphan Hydrochloride (13a). Compound **13a** was prepared as described for **12a** starting with racemic **33** and *S*-(−)-2-benzyloxypropionyl chloride. The desired diastereomer was obtained by recrystallization from 2-propanol; mp 244−246 °C; $[\alpha]_D^{20}$ = +11.8° (c 1.0, MeOH). ^{1}H NMR (CD_3OD): δ 1.32 (d, 3H, J = 5.8 Hz), 1.43 (s, 3H), 1.40−3.80 (m, 11 H), 3.98 (m, 1H), 4.50 (d, 1H, J = 11.6 Hz), 4.75 (d, 1H, J = 11.6 Hz), 6.68 (d, 1H, J = 7.9 Hz), 6.85 (d, 1H, J = 7.9 Hz), 7.05 (t, 1H, J = 7.9 Hz), 7.26−7.48 (m, 5H). Anal. ($C_{23}H_{29}NO_2$·HCl) C, H, N.

X-ray Structure Determination of 9a. Crystals were grown by recrystallization from a mixture of methanol and *tert*-butyl methyl ether, which diffused into each other. A crystal of the dimensions 0.30 × 0.30 × 0.30 mm^3 was mounted on a glass fiber. All measurements were made on a Rigaku AFC7 diffractometer with graphite monochromated Cu K radiation on a Rigaku RU200 rotating anode generator. Twenty reflections with 43° ≤ θ ≤ 62° were used to determine the cell parameters. Reflections (3390) were collected of which 1695 were independent (R_{int} = 4.9%) and 2851 (including Friedel pairs) were observed ($I > 3.0\sigma(I)$), which were used for the structure analysis. Azimuthal scans of several reflections indicated no need for an empirical absorption correction. The structure was solved by direct methods.[49] The refinement of the structure parameters was by least-squares methods (function minimized, $\sum w (|F_o| - |F_c|)^2$ where $w = [1/(\sigma^2(F_o))] = [\sigma_c^2(F_o) + [(p^2)/4]\ F_o^2]^{-1}$, $\sigma_c(F_o)$ = esd based on counting statistics, p = 0.007, 262 parameters; hydrogen atoms were included but not refined; S = 2.77, R_1 = 0.037, and R_w = 0.043; largest difference peak, 0.42 e/Å^3; largest difference hole, −0.14 e/Å^3. All calculations were done with the teXsan programs.[50] The absolute configuration was determined as 1*R*,2″*S* using information derived from measured and calculated intensity differences of Bijvoet reflections as implemented in teXsan. Crystal data $C_{25}H_{34}NO_2Cl$: M_r = 416.00, orthorhombic, $P2_12_12_1$, a = 12.999(4) Å, b = 19.246(4) Å, c = 9.180(3) Å, V = 2296.7(8) Å^3, Z = 4, D_x = 1.203 g/cm^3, λ(Cu Kα) = 1.5418 Å, μ = 16.21 cm^{-1}, $F(000)$ = 896, and T = 293 K.

X-ray Structure Determination of 13a. The analysis was performed in analogy to **9a**. A crystal of the dimensions 0.40 × 0.20 × 0.20 mm^3 was used. Reflections (1563) were collected, and 1304 were observed ($I > 3.0\sigma(I)$), which were used for the structure analysis. An empirical absorption correction was applied based on azimuthal scans of several reflections (transmission factors from 0.90 to 1.00). Refinement, p = 0.003, 244 parameters; hydrogen atoms were included but not refined; S = 3.59, R_1 = 0.039, and R_w = 0.043; largest difference peak, 0.19 e/Å^3; largest difference hole, −0.14 e/Å^3. The absolute configuration of the molecule was deduced on the basis of the known absolute stereochemistry of 2″. Crystal data $C_{23}H_{30}NO_2Cl$: M_r = 387.95, orthorhombic, $P2_12_12_1$, a = 12.970(1) Å, b = 17.982(1) Å, c = 9.004(2) Å, V = 2099.9(5) Å^3, Z = 4, D_x = 1.227 g/cm^3, λ(Cu Kα) = 1.5418 Å, μ = 17.36 cm^{-1}, $F(000)$ = 832, and T = 293 K.

In Vitro Binding. [^{3}H]BTX-B (tritiated BTX-A-20-a-benzoate) binding was measured in synaptosomal preparations of rat cerebral cortex. Membrane suspensions were incubated for 1 h at 37 °C with 1 nmol/L [^{3}H]BTX-B in incubation buffer (130 mM choline Cl/50 mM HEPES-Tris, pH 7.4/5.5 mM glucose/5.4 mM KCl/0.8 mM $MgSO_4$) in the presence of 10−50 μL of scorpion venom (10 mg/mL in water) depending on the maximal specific binding of [^{3}H]BTX-B. Nonspecific binding was determined by the addition of 100 μmol/L aconitine. Incubation was terminated by rapid vacuum filtration through glass fiber filter (type G-7 ICH-201 Inotech) and washing twice with buffer (163 mM choline Cl/50 mM HEPES-Tris, pH 7.4/1.8 mM $CaCl_2$/1.8 mM $MgSO_4$). Binding experiments at the dihydropyridine site, the diltiazem site, and the verapamil site of the L type calcium channel were performed in the laboratory of Cerep (Le Bois lÉvêque, France).

Veratridine-Induced Glutamate Release. The assay followed procedures reported[51,52] with some modifications. Cross-chopped slices, 0.2 mm thick, from rat brain cortex or striatum (strain Chbb:Thom) were prepared and preincubated at 37 °C for 45 min in Krebs−Henseleit buffer (in mM: NaCl 120, KCl 4.8, $CaCl_2$ 1.3, KH_2PO_4 1.2, $MgSO_4$ 1.2, $NaHCO_3$ 25, pH 7.4). In addition, the buffer contained 2 g of glucose, 100 mg of ethylenediaminetetraacetic acid, and 200 mg of ascorbic acid per liter. The medium was continuously saturated with 95% O_2/5% CO_2 and changed completely three times during this preincubation period. Slices randomly distributed in microcentrifuge tubes (equivalent to about 430 μg of protein) were then incubated for 15 min with (stimulated) or without (basal) 3 μM veratridine using an Eppendorf model 5437 Thermomixer (Eppendorf, Hamburg, Germany). The test drug was present throughout the incubation period or absent in the controls. Incubation was terminated by centrifugation with 16 000*g* for 5 min in an Eppendorf model 5415C centrifuge. The supernatant was used for glutamate determination by means of high-performance liquid chromatography and fluorimetric detection.[53] Protein was determined according to the Coomassie Blue procedure.[54]

MES Test. This assay was performed as previously described.[55] Different doses of test compounds were administered via sc injection to groups of 10 male OF1 mice. The electroshock (20 mA/50 Hz/200 ms) via eye electrodes was applied 15 min after injection of the test compound. The percentage of animals that did not develop tonic convulsions was determined. The dose required to inhibit tonic seizures by 50% (ID_{50}) was calculated by log-probit analysis from three to four different doses of each test compound.

Acknowledgment. We thank Hanfried Baltes, Rainer Fröhlich, Holger Werle, Stephan Kurtze, and Elisabeth Weghofer for their excellent technical assistance as well as Dr. Wolfgang Tröger and Wolfgang Pryss (Department of Analytics, Boehringer Ingelheim Pharma KG) for providing spectral data. We are grateful to Dr. Rainer Palluk (Department of Drug Safety, Boehringer Ingelheim GmbH) and Gisela Mengeling for their support with MES data.

References

(1) Mattson, M. P.; Mark, R. J. In *Excitotoxicity and Excitoprotection In Vitro*; Siesjö, B. K., Wieloch, T., Eds.; Advances in Neurology, Vol. 71, Cellular and Molecular Mechanisms of Ischemic Brain Damage; Lippincott-Raven Publishers: Philadelphia, 1996; pp 1−35.

(2) Tymianski, M.; Tator, C. H. Normal and abnormal calcium homeostasis in neurons: a basis for the pathophysiology of traumatic and ischemic central nervous system injury. *Neurosurgery* **1996**, *38*, 1176−1195.

(3) Szatkowski, M.; Barbour, B.; Attwell, D. Nonvesicular release of glutamate from glial cells by reversed electrogenic glutamate uptake. *Nature* **1990**, *348*, 443−446.

(4) Stys, P. K.; Waxman, S. G.; Ransom, B. R. Ionic Mechanism of Anoxic Injury in Mammalian CNS White Matter: Role of Na^+ Channels and Na^+−Ca^{2+} Exchanger. *J. Neurosci.* **1992**, *12*, 430−439.

(5) Stys, P. K. Anoxic and Ischemic Injury of Myelinated Axons in CNS White Matter: From Mechanistic Concepts to therapeutics. *J. Cereb. Blood Flow Metab.* **1998**, *18*, 2−25.

(6) Taylor, C. P.; Narasimhan, L. S. Sodium channels and therapy of central nervous system diseases. *Adv. Pharmacol.* **1997**, *39*, 47−98.

(7) Taylor, C. P.; Meldrum, B. S. Na^+ channels as targets for neuroprotective drugs. *Trends Pharmacol. Sci.* **1995**, *16*, 309−316.

(8) Urenjak, J.; Obrenovitch, T. P. Pharmacological modulation of voltage-gated Na^+ channels: A rational and effective strategy against ischemic brain damage. *Pharmacol. Rev.* **1996**, *48*, 21−58.

(9) Hartshorne, R. P.; Catterall, W. A. The sodium channel from rat brain. *J. Biol. Chem.* **1983**, *259*, 1667−1675.

(10) Catterall, W. A. Structure and function of voltage-sensitive ion channels. *Science* **1988**, *242*, 50−61.

(11) Catterall, W. A. Common modes of drug action on Na^+ channels: local anesthetics, antiarrhythmics and anticonvulsants. *Trends Pharmacol. Sci.* **1987**, *8*, 57−65.
(12) Catterall, W. A. Neurotoxins that act on voltage-sensitive sodium channels in excitable membranes. *Annu. Rev. Pharmacol. Toxicol.* **1980**, *20*, 15−43.
(13) Catterall, W. A. Cellular and molecular biology of voltage-gated sodium channels. *Physiol. Rev.* **1992**, *72*, S15−S48.
(14) Catterall, W. A. Structure and function of voltage-gated ion channels *Annu. Rev. Biochem.* **1995**, *65*, 493−531.
(15) Isom, L. L.; De Jongh, K. S.; Patton, D. E.; Reber, B. F. X.; Offord, J.; Charbonneau, H.; Walsh, K.; Goldin, A. L.; Catterall, W. A. Primary structure and functional expression of the α1 subunit of the rat brain sodium channel. *Science* **1992**, *256*, 839−842.
(16) Isom, L. L.; Ragsdale, D. S.; De Jongh, K. S.; Westenbrock, R. E.; Reber, B. F. X.; Scheuer, T.; Catterall, W. A. Structure and function of the β2 subunit of brain sodium channels, a transmembrane glycoprotein with a CAM motif. *Cell* **1995**, *83*, 433−442.
(17) Gautron, S.; Santos, G. D.; Pinto-Henrique, D.; Koulakoff, A.; Gros, F.; Berwald-Netter, Y. The glial voltage-gated sodium channel: cell- and tissue-specific mRNA expression. *Proc. Natl. Acad. Sci. U.S.A.* **1992**, *89*, 7272−7276.
(18) Kayano, T.; Noda, M.; Flockerzi, V.; Takahashi, H.; Numa, S. Primary structure of rat brain sodium channel III deduced from the cDNA sequence. *FEBS Lett.* **1988**, *228*, 187−194.
(19) Noda, M.; Ikeda, H.; Kayano, T.; Suzuki, H.; Takeshima, H.; Kurasaki, M.; Takahashi, H.; Numa, S. Existence of distinct sodium channel messenger RNAs in rat brain. *Nature* **1986**, *320*, 188−192.
(20) Schaller, K. L.; Krzemien, D. M.; Yarowsky, P. J.; Krueger, B. K.; Caldwell, J. H. A novel, abundant sodium channel expressed in neurons and glia. *J. Neurosci.* **1995**, *15*, 3231−3242.
(21) Yarowski, P. J.; Krueger, B. K.; Olson, C. E.; Clevinger, E. C.; Koos, R. D. Brain and heart sodium channel subtype mRNA expression in rat cerebral cortex. *Proc. Natl. Acad. Sci. U.S.A.* **1991**, *88*, 9453−9457.
(22) Catterall, W. A. Cellular and molecular biology of voltage-gated sodium channels. *Physiol. Rev.* **1992**, *72*, S15−S48.
(23) Gordon, D. *Toxins and Signal Transduction*; Gutman, Y., Strichartz, G. R., Eds.; Harwood: London, 1990; pp 119−149.
(24) Satin, J.; Limberis, J. T.; Kyle, J. W.; Rogart, R. B.; Fozzard, H. A. The saxitoxin/tetrodotoxin binding site on cloned rat brain Iia Na channels is in the transmembrane electric field. *Biophys. J.* **1994**, *67*, 1007−1014.
(25) Catterall, W. A. Activation of the action potential Na^+ ionophore by neurotoxins. An allosteric model. *J. Biol. Chem.* **1977**, *252*, 8669−8676.
(26) Catterall, W. A.; Morrow, C. S.; Daly, J. W.; Brown, G. B. Binding of batrachotoxin A 20-α-benzoate to a receptor site associated with sodium channels in synaptic nerve ending particles. *J. Biol. Chem.* **1981**, *256*, 8922−8927.
(27) Albuquerque, E. X.; Daly, J. W.; Witcop, B. Batrachotoxin: chemistry and pharmaclogy. *Science* **1971**, *172*, 995−1002.
(28) Wang, S. Y.; Wang, G. K. Point mutations in segment I−S6 render voltage-gated Na^+ channels resistant to batrachotoxin. *Proc. Natl. Acad. Sci. U.S.A.* **1998**, *95*, 2653−2658.
(29) Linford, N. J.; Cantrell, A. R.; Qu, Y.; Scheuer, T.; Catterall, W. A. Interaction of batrachotoxin with the local anesthetic receptor site in transmembrane segment IVS6 of the voltage-gated sodium channel. *Proc. Natl. Acad. Sci. U.S.A.* **1998**, *95*, 13947−13952.
(30) Graham, S. H.; Chen, J.; Lan, J.; Leach, M. J.; Simon, R. P. Neuroprotective effects of a use-dependent blocker of voltage-dependent sodium channels, BW619C89, in rat middle cerebral artery occlusion. *J. Pharmacol. Exp. Ther.* **1994**, *269*, 854−859.
(31) Leach, M. J.; Swan, J. H.; Eisenthal, D.; Dopson, M.; Nobbs, M. BW619C89, a glutamate release inhibitor, protects against focal cerebral ischemic damage. *Stroke* **1993**, *24*, 1063−1067.
(32) Kucharczyk, J.; Mintorovitch, J.; Moseley, M. E.; Asgari, H. S.; Sevick, R. J.; Derugin, N.; Norman, D. Ischemic brain damage: Reduction by sodium−calcium ion channel modulator RS-87476. *Radiology* **1991**, *179*, 221−227.
(33) Alps, B. J.; Calder, C.; Wilson, A. D.; McBean, D. E.; Armstrong, J. M. Reduction by lifarizine of the neuronal damage induced by cerebral ischaemia in rodents. *Br. J. Pharmacol.* **1995**, *115*, 1439−1446.
(34) May, G. R.; Rowand, W. S.; McCormack, J. G.; Sheridan, R. D. Neuroprotective profile of lifarizine (RS-87476) in rat cerebrocortical neurones in culture. *Br. J. Pharmacol.* **1995**, *114*, 1365−1376.
(35) McBean, D. E.; Winters, V.; Alasdair, D. W.; Oswald, C. B.; Alps, B. J.; Armstrong, J. M. Neuroprotective efficacy of lifarizine (RS-87476) in a simplified rat survival model of 2 vessel occlusion. *Br. J. Pharmacol.* **1995**, *116*, 3093−3098.
(36) Aronowski, J.; Strong, R.; Grotta, J. C. Combined neuroprotection and reperfusion therapy for stroke. Effect of lubeluzole and Diaspirin cross-linked hemoglobin in experimental focal ischemia. *Stroke* **1996**, *27*, 1571−1577.
(37) DeRyck, D.; Keersmaekers, R.; Dytschaever, H.; Claes, C.; Clincke, G.; Janssen, M.; Van Reet, G. lubeluzole protects sensorimotor function and reduces infarct size in a photochemical stroke model in rats. *J. Pharmacol. Exp. Ther.* **1996**, *279*, 748−758.
(38) Haseldonckx, M.; Van Reempts, J.; Van de Ven, M.; Wouters, L.; Borgers, M. Protection with lubeluzole against delayed ischemic brain damage in rats. *Stroke* **1997**, *28*, 428−432.
(39) Squire, I. B.; Lees, K. R.; Pryse-Phillips, W.; Kertesz, A.; Bamford, J. The effects of lifarizine in acute cerebral infarction: a pilot safety study. *Cerebrovasc. Dis.* **1996**, *6*, 156−160.
(40) Carter, A. J. The importance of voltage-dependent sodium channels in cerebral ischaemia. *Amino Acids* **1998**, *14*, 159−169.
(41) Netzer, R.; Pflimlin, P.; Trube, G. Dextromethorphan blocks *N*-methyl-D-aspartate-induced currents and voltage-operated inward currents in cultured cortical neurons. *Eur. J. Pharmacol.* **1993**, *238*, 209−216.
(42) Trube, G.; Netzer, R. Dextromethorphan: cellular effects reducing neuronal hyperactivity. *Epilepsia* **1994**, *35*, S62−S67.
(43) Grauert, M.; Bechtel, W. D.; Ensinger, H. A.; Merz, H.; Carter, A. J. Synthesis and Structure−Activity Relationships of 6,7-Benzomorphan Derivatives as Antagonists of the NMDA Receptor-Channel Complex. *J. Med. Chem.* **1997**, *40*, 2922−2930.
(44) Carter, A. J.; Grauert, M.; Pschorn, U.; Bechtel, W. D.; Bartmann-Lindholm, C.; Qu, Y.; Scheuer, T.; Catterall, W. A.; Weiser, T. Potent blockade of sodium channels and protection of brain tissue from ischemia by BIII 890 CL. *Proc. Natl. Acad. Sci. U.S.A.* **2000**, *97*, 4944−4949.
(45) Danysz, W.; Parsons, C. G.; Bresink, I.; Quack, G. A revived target for drug development? Glutamate in CNS disorders. *Drug News Perspect.* **1995**, *8*, 261−277.
(46) Small, D. L. Ion channels involved in stroke. *Emerging Ther. Targets* **2001**, *5*, 59−86.
(47) Stys, P. K.; Waxman, S. G.; Ransom, B. R. Ionic mechanisms of anoxic injury in mammalian CNS white matter: role of Na^+ channels and Na^+/Ca^{2+} exchanger. *J. Neurosci.* **1992**, *12*, 430−439.
(48) Grauert, M.; Rho, J. M.; Subramaniam, S.; Rogawski, M. A. *N*-methyl-D-aspartate receptor channel block by the enantiomeric 6,7-benzomorphans BIII 277 CL and BIII 281 CL. *J. Pharmacol. Exp. Ther.* **1998**, *285*, 767−776.
(49) Sheldrick, G. M. *Crystallographic Computing 3*; Sheldrick, G. M., Kruger, C., Goddard, R., Eds.; Oxford University Press, 1985; pp 175−189.
(50) *Crystal Structure Analysis Package*; Molecular Structure Corporation, 1985 and 1992.
(51) Leach, M. J.; Marsden, C. M.; Miller, A. A.; O'Donnell, R. A.; Weston, S. B. Changes in cortical amino acids during electrical kindling in rats. *Neuropharmacology* **1985**, *24*, 937−940.
(52) Meldrum, B. S.; Swan, J. H.; Leach, M. J.; Millan, M. H.; Gwinn, R.; Kadota, K.; Graham, S. H.; Chen, J.; Simon, R. P. Reduction of glutamate release and protection against ischemic brain damage by BW 1003C87. *Brain Res.* **1992**, *593*, 1−6.
(53) Kehr, J. Determination of gutamate and aspartate in microdialysis samples by reversed-phase column liquid chromatography with fluorescence and electrochemical detection. *J. Chromatogr. B Biomed. Appl.* **1998**, *708*, 27−38.
(54) Bradford, M. M. A rapid and sensitive method for the quantitation of microgram quantities of protein utilizing the principle of protein-dye binding. *Anal. Biochem.* **1976**, *72*, 248−254.
(55) Weiser, T.; Brenner, M.; Palluk, R.; Bechtel, W. D.; Ceci, A.; Brambilla, A.; Ensinger, H. A.; Sagrada, A.; Wienrich, M. BIIR 561 CL: A Novel Combined Antagonist of α-Amino-3-hydroxy-5-methyl-4-isoxazolepropionic Acid Receptors and Voltage-Dependent Sodium Channels with Anticonvulsive and Neuroprotective Properties. *J. Pharmacol. Exp. Ther.* **1999**, *289*, 1343−1349.

JM020875J